SLAC – PUB – 3707
June 1985
(T)

EVOLUTION OF RELATIVISTIC MULTIQUARK SYSTEMS*

STANLEY J. BRODSKY AND CHUENG–RYONG JI

Stanford Linear Accelerator Center
Stanford University, Stanford, California, 94305

ABSTRACT

The short-distance behavior of multiquark wavefunctions can be systematically computed in perturbative QCD. In this paper we analyze the wavefunction of a four-quark color-singlet bound state in $SU(2)_C$ as an analogue to the six-quark problem in QCD. We first solve the QCD evolution equation for the multi-quark distribution amplitude at short distances in the basis of completely antisymmetrized quark representations. The eigensolutions of the evolution kernel correspond to a spectrum of candidate states of the relativistic multi-quark system. We then connect the four-quark antisymmetric representations and the eigensolutions to the physical two-cluster basis of $SU(2)_C$ dibaryon (NN, $N\Delta$, $\Delta\Delta$) and hidden color (CC) components and derive constraints on the effective nuclear potential between two clusters. We also find anomalous states in the spectrum which cannot exist without substantial hidden-color degrees of freedom.

Submitted to *Physical Review D*

* Work supported by the Department of Energy, contract DE – AC03 – 76SF00515.

1. INTRODUCTION

Among the key goals in the application of quantum chromodynamics (QCD) to nuclear physics are to predict the bound-state spectrum of relativistic multi-quark color-singlet systems and to identify the role of non-nucleonic degrees of freedom in a nucleus. Recently, we presented a general method for solving the QCD evolution equations for distribution amplitudes, the equations which determine the behavior of hadron wavefunctions at short distances. An important simplification of the analysis is to choose as a basis of the evolution kernel the set of antisymmetrized multi-quark representations. Since the evolution equation is relativistic and obeys all the conservation laws and symmetries of the full QCD Lagrangian, its set of eigensolutions should correspond closely to the structure of the true spectrum. Applications of the method to the baryon system have been presented in Ref. 1.

In this paper, we analyze the structure of the spectrum and the short-distance behavior of the four-quark system in $SU(2)_C$ as a first attempt in analyzing actual multiquark color-singlet bound states in QCD. Even though this is a toy model, the results have a number of interesting implications for the realistic dibaryon system.

An outline of the method is as follows: we first construct the set of completely antisymmetric four-quark representations as a basis for diagonalizing the QCD evolution kernel. After diagonalizing the mixing matrices, we find the eigenvalues and the eigensolutions of the four-quark evolution equation. The eigenvalues are the anomalous dimensions of the distribution amplitudes which describe the short distance behavior of the system. The eigensolutions correspond to candidate four-quark states for the spectrum of the full $SU(2)_C$ Hamiltonian.

A relativistic color-singlet bound state in QCD has a consistent Fock representation at equal time on the light cone in A^+ gauge. The lowest Fock amplitude is referred to as the valence wavefunction. In the evolution equation formalism,[2] the valence wavefunction is represented by the distribution amplitude $\phi(x_i, Q)$, the amplitude for the valence quanta to each carry light-cone longitudinal momentum fraction

$$x_i = \frac{k_i^+}{\sum_{i=1}^4 k_i^+} = \frac{k_i^0 + k_i^3}{\sum_{i=1}^4 (k_i^0 + k_i^3)},$$

collinear in relative transverse momenta up to the scale Q. Physically, $\phi(x_i, Q)$ at large Q^2 probes the short-distance behavior of the quark system, in the regime where all the constituents are within a transverse distance $1/Q$ of each other. In general, the logarithmic Q^2 dependence for $\phi(x_i, Q)$ is predicted by QCD from the anomalous dimensions (eigenvalues) of the evolution equation.

The four-quark eigensolutions can be expanded on the physical basis of effective clusters, the analogs of the NN, $\Delta\Delta$, $N\Delta$, and CC states in QCD. By analyzing the behavior of $\phi(x_i, Q)$ at large Q^2, we can predict the effective potential between two clusters. For example, we find that one of the hidden color states has a large projection on the eigensolution with leading anomalous dimension (dominant at short distances), whereas the states analogous to NN and $\Delta\Delta$ in QCD have an almost negligible leading component. This implies that the effective potential tends to be repulsive between color-singlet clusters and attractive between colored clusters at short distance.

We also find two other types of four-quark states in $SU(2)$ color which cannot be identified with dibaryon degrees of freedom. One of these states has equal NN, $\Delta\Delta$ and CC components. The other state is an anomalous hidden-

color two-cluster system orthogonal to the usual hidden-color state which has the unusual feature that it has very small projection on the eigensolutions which dominate at short distance; i.e the effective potential between the colorful clusters of the anomalous hidden color state tends to be repulsive. We speculate that the analogous anomalous states in QCD could be quasi-stable non-nucleonic nuclear systems, possibly related to the anomalous phenomena apparently observed in nuclear collisions.[3,4] These results also give some support to the conjecture that multiquark hidden color components exist in ordinary nuclei.[4]

The organization of this paper is as follows: In Section 2, antisymmetric four quark representations are constructed. In Section 3, the four quark evolution equation is expanded on this basis and solved. In Section 4, we relate the eigensolutions to an effective cluster representation and derive constraints on the nuclear potential between two clusters. In Section 5, we discuss the anomalous states of the $SU(2)_C$ theory. The results and conclusions are summarized in Section 6.

2. ANTISYMMETRIC REPRESENTATIONS

In Ref. 1 we presented a general method for constructing antisymmetric representations of relativistic many-fermion systems at equal time on the light-cone and used it to solve the evolution equation in QCD for the three quark system.[2] Essentially, we use the following procedure:.

1. Construct the irreducible representations in each quantum space, color (C), isospin (T), spin (S) and orbital (O) in terms of the irreducible representations of the permutation group by using the Young diagram technique.[5]

For the orbital representations, we use the index-power space which is constructed from the powers n_i of the longitudinal momentum fractions x_i. The orbital representations for the ℓ quark system are the polynomials $\prod_{i=1}^{\ell} x_i^{n_i}$ with the orthonormalization condition,

$$\int [dx]\ \omega(x_i)\ \phi_m^*(x_i)\ \phi_n(x_i) = \delta_{mn}, \tag{2.1}$$

where ϕ_n and ϕ_m are the orbital representations constructed by the same Young diagram with the index-power n and m, and $\omega(x_i) = \prod_{i=1}^{\ell} x_i$.

2. Construct completely antisymmetric representations in the entire $CTSO$ space from the inner product of Young diagrams, using the Clebsch-Gordan coefficients of the S_ℓ permutation group.

The color singlet state of the four-quark system in $SU(2)_C$ is given by the Young diagram $\begin{array}{|c|c|}\hline \ & \ \\ \hline \ & \ \\ \hline \end{array}$. There are two orthogonal representations given by

$$\begin{array}{|c|c|}\hline b & b \\ \hline w & w \\ \hline \end{array} = \begin{cases} \begin{array}{|c|c|}\hline 1 & 3 \\ \hline 2 & 4 \\ \hline \end{array} = \dfrac{1}{\sqrt{2}}\ (\varsigma_1 - \varsigma_2) \\ \\ \begin{array}{|c|c|}\hline 1 & 2 \\ \hline 3 & 4 \\ \hline \end{array} = -\dfrac{1}{\sqrt{6}}\ (\varsigma_1 + \varsigma_2 - 2\varsigma_3), \end{cases} \tag{2.2}$$

where

$$\varsigma_1 = \frac{1}{\sqrt{2}}(bwbw + wbwb)$$
$$\varsigma_2 = \frac{1}{\sqrt{2}}(wbbw + bwwb)$$

and

$$\varsigma_3 = \frac{1}{\sqrt{2}}(bbww + wwbb) \quad . \tag{2.3}$$

Note that unlike the three quark system in QCD which has a unique antisym-

metric color representation, the $SU(2)_C$ multiquark system has mixed color symmetry; i.e., several orthogonal representations.

The notation used in Eq. (2.3) can be repeated for isospin and spin. We denote these representations by T_1, T_2, and T_3 (S_1, S_2, and S_3) for $T = 0$ ($S = 0$) with the substitution of (b, w) by (u, d) $((\uparrow, \downarrow))$. Also we use the conjugate notation $\overline{T}_1$, $\overline{T}_2$, and $\overline{T}_3$ ($\overline{S}_1$, $\overline{S}_2$ and $\overline{S}_3$) with the "–" sign instead of "+" sign between the two terms in the respective representations for the $(T,\ T_Z) = (1,0)$ $((S,\ S_Z) = (1,0))$ states. In this analysis, we consider the $T = 0$ case, the analogue to the actual deuteron system.

The results of the four-quark antisymmetric representations are summarized in Table I. For convenience, we present only effective representations which are sufficient to show the operation of the evolution kernel. In the $S_Z = 0$ case, the S_1T_2 and $\overline{S}_1T_2$ terms are presented for $S = 0$ and 1 representations, respectively. In the $S_Z = 1$ and 2 cases the $(\uparrow\uparrow\uparrow\downarrow)T_1$ and $(\uparrow\uparrow\uparrow\uparrow)T_1$ terms are presented, respectively. Also, we denote in parentheses in Table I the spin-orbit Young diagrams for the cases in which several spin-orbit total symmetries are allowed from the inner product of spin and orbit representations.

3. EVOLUTION OF THE FOUR-QUARK SYSTEM

The distribution amplitude $\phi(x_i, Q)$ is the valence Fock State wave function at equal time on the light cone integrated over transverse momenta $\vec{k}_{\perp i}^2 \lesssim Q^2$:

$$\phi(x_i, Q) = \int^Q \left(\prod_{i=1}^4 \frac{d^2\vec{k}_{\perp i}}{16\pi^3} \right) 16\,\pi^3\delta^2\left(\sum_i \vec{k}_{\perp i} \right) \psi^Q(x_i, \vec{k}_{\perp i}) \,. \qquad (3.1)$$

The wave function $\psi^Q(x_i, \vec{k}_{\perp i})$ satisfies the Bethe-Salpeter type bound state wave equation shown in Fig. 1. One can derive an evolution equation for the four-quark

color-singlet state which expresses the variation of $\phi(x_i, Q)$ as Q^2 is increased:

$$\left(\frac{\partial}{\partial \xi} + \frac{2C_F}{\beta}\right) \widetilde{\phi}(x_i, Q) = -\frac{2}{\beta} \int [dy] V(x_i, y_i) \widetilde{\phi}(y_i, Q) \ , \tag{3.2}$$

where

$$\xi(Q^2) = \frac{\beta}{4\pi} \int_{Q_0^2}^{Q^2} \frac{dk_\perp^2}{k_\perp^2} \ \alpha_s(k_\perp^2) \ , \tag{3.3}$$

$$\phi(x_i, Q) = x_1 x_2 x_3 x_4 \ \widetilde{\phi}(x_i, Q), \tag{3.4}$$

and $\beta = 11 - \frac{2}{3} n_f$ (n_f is the number of flavors) and $C_F = (n_c^2 - 1)/2n_c$ (=3/4 in $SU(2)_C$). The term $\frac{2C_F}{\beta}$ in Eq. (3.2) is derived from the wavefunction renormalization of the quark propagators. To leading order in $\alpha_s(Q^2)$, $V(x_i, y_i)$ is computed from the single-gluon exchange kernel and is given by

$$\begin{aligned} V(x_i, y_i) = & \sum_{i \neq j} \left(\frac{\vec{\tau}_i}{2} \cdot \frac{\vec{\tau}_j}{2}\right) \theta(y_i - x_i) \prod_{k \neq i,j} \delta(x_k - y_k) \\ & \times \frac{y_j}{x_j} \left(\frac{\delta_{h i \bar{h}_j}}{x_i + x_j} + \frac{\Delta}{y_i - x_i}\right) \\ & = V(y_i, x_i) \ , \end{aligned} \tag{3.5}$$

where $\vec{\tau} = (\tau_1, \ \tau_2, \ \tau_3)$ are the $SU(2)_C$ Pauli matrices and $\delta_{h i \bar{h}_j} = 1(0)$ when the constituents $\{i, j\}$ have antiparallel (parallel) helicities. The infrared singularity in the kernel at $x_i = y_i$ cancels for color singlet bound states: $\Delta\widetilde{\phi}(y_i, Q) = \widetilde{\phi}(y_i, Q) - \widetilde{\phi}(x_i, Q)$.

The general solution of Eq. (3.2) can be written in the form

$$\widetilde{\phi}(x_i, Q) = \sum_{n=0}^{\infty} a_n \ \widetilde{\phi}_n(x_i) e^{-\gamma_n \xi(Q^2)} \ , \tag{3.6}$$

where γ_n and $\widetilde{\phi}_n$ are the eigenvalues and eigensolutions of the following charac-

teristic equation:

$$\left(\frac{2C_F}{\beta} - \gamma_n\right) \widetilde{\phi}_n(x_i) = -\frac{2}{\beta} \int_0^1 [dy]\ V(x_i, y_i) \widetilde{\phi}_n(y_i)\ . \tag{3.7}$$

The $\widetilde{\phi}_n$ basis is given in Table I, as explained in the last section. The remaining task is to find the anomalous dimensions γ_n which determine the short-distance behavior of the four-quark wave function by computing the matrix of the evolution kernel in this basis and diagonalizing it. Note that when a gluon is exchanged between the first and second quarks then the basis vectors ς_1 and ς_2 can be interchanged while ς_3 preserves itself. Thus the calculation of the color factors is not as simple as the three-quark QCD case and requires a complete matrix analysis.

The mixing between different spin and orbital multiplets is similar to the three-quark case. For example, the mixing matrix for the orbital power $n = 2$ has dimension 4×4 for the $S_Z = 1$ case and dimension 6×6 for the $S_Z = 0$. After diagonalizing the mixing matrices, we find the eigenvalues γ_n and the eigensolutions $\widetilde{\phi}_n$. The results are summarized in Table II.

4. TWO-CLUSTER DECOMPOSITION

In this chapter, we will connect the eigensolutions of the four-quark evolution equation to the physical two-cluster basis and derive constraints on the effective nuclear potential between the clusters.

The four-quark antisymmetric representations can always be decomposed into a sum of products of pairs of two-quark representations. The two-quark antisymmetric representation is called a cluster which is classified according to its quantum numbers under $G = SU(2)_C \times SU(2)_T \times SU(2)_S$. In $SU(2)_C$ a four-quark

color singlet can be constructed not only from a pair of two-quark color singlet, but also from the product of two-quark color triplets (C). These correspond to dibaryon and hidden color states, respectively. The dibaryon states are classified by their isospin quantum numbers : N and Δ correspond to $T = 0$ and 1, in analogy to the $T = 1/2$ and $3/2$ states in QCD.

A given four-quark antisymmetric representation (A) can be decomposed onto two clusters ($A_1 \otimes A_2$) using the following steps:

1. Represent the four-quark antisymmetric representation as an inner product form $A = C \times T \times S \times O$.

2. Decompose each four-quark representations C, T, S and O as an outer product of two two-quark representations using fractional parentage coefficients,[6] e.g. $C = C_1 \otimes C_2$.

3. Recombine the representations as an inner product: $A = (C_1 \otimes C_2) \times (T_1 \otimes T_2) \times (S_1 \otimes S_2) \times (O_1 \otimes O_2)$.

4. Commute the order of inner product and outer product, gathering together representations of the same cluster: $A = (C_1 \times T_1 \times S_1 \times O_1) \otimes (C_2 \times T_2 \times S_2 \times O_2) \equiv A_1 \otimes A_2$.

5. It is sufficient to consider only the coefficient of the symmetric orbitals O_1 and O_2 to classify the clusters such as NN, $N\Delta$, $\Delta\Delta$ and CC.

Using these steps, we can determine the relation between antisymmetrized four-quark antisymmetric representations and the effective two-cluster representations. For the $T = S = 0$ case, we obtain the transition table given in Table III which relates the two kinds of representations. M. Harvey[7] has already obtained the analogous transformation matrices between the physical basis and the

symmetry basis for six-quark systems. His definitions of the physical and symmetry bases are essentially the same as the two-cluster representations and the completely antisymmetric representations used here.

From Table III, we can relate the two-cluster distribution amplitudes with the completely antisymmetric quark distribution amplitudes. For example, the dinucleon distribution amplitude is given by

$$\begin{aligned}\phi_{NN}(x_i,Q) = &-\frac{1}{2}\,\phi_{[4]\{22\}}\,(x_i,Q) + \frac{1}{2}\,\phi_{[22]\{22\}}(x_i,Q) \\ &-\frac{1}{\sqrt{2}}\,\phi_{[22]\{4\}}(x_i,Q)\ ,\end{aligned} \tag{4.1}$$

where the orbital and the spin-isospin symmetries are represented inside the square and the curly brackets. Since the eigensolutions are linear combinations of completely antisymmetric representations, we can relate the right-hand side of Eq. (4.1) with the eigensolutions given by Table II. The eigensolutions $\phi_{\gamma_n}(x_i,Q)$ have the following form:

$$\phi_{\gamma_n}(x_i,Q) = e^{-\gamma_n \xi(Q^2)}\ \phi_{\gamma_n}(x_i)\ . \tag{4.2}$$

Consequently, we can expand each two-cluster distribution amplitudes in terms of the orbital index power representations $\phi_{\gamma_n}(x_i)$. To probe the high Q^2 behavior of the two-cluster distribution amplitudes, it is sufficient to consider only the leading terms which have the lowest anomalous dimensions γ_n because of the damping factor of Eq. (4.2). The lowest orbital power with representations which provide well-defined two-cluster distribution amplitudes is $n = 2$. We will discuss the special properties of the $n = 0$ representation in the next section.

The $n = 2$ two-cluster distribution amplitudes can be expanded in terms of the orbital representations $\phi_{\gamma_2}(x_i) \equiv \phi_{\gamma_2}$:

$$\begin{aligned}\phi_{NN}(x_i, Q) = 0.07\ e^{0.13\widetilde{\xi}}\ \phi_{0.13} - 0.64\ e^{-0.06\widetilde{\xi}}\phi_{-0.06} \\ + 0.39\ e^{-2.01\widetilde{\xi}}\ \phi_{-2.01} - 0.47\ e^{-5.50\widetilde{\xi}}\phi_{-5.50} \\ + 0.44\ e^{-6.75\widetilde{\xi}}\ \phi_{-6.75} + 0.15\ e^{-7.40\widetilde{\xi}}\phi_{-7.40}\ ,\end{aligned} \tag{4.3a}$$

$$\begin{aligned}\phi_{\Delta\Delta}(x_i, Q) = -0.07\ e^{0.13\widetilde{\xi}}\ \phi_{0.13} - 0.59\ e^{-0.06\widetilde{\xi}}\phi_{-0.06} \\ + 0.32\ e^{-2.01\widetilde{\xi}}\ \phi_{-2.01} + 0.47\ e^{-5.50\widetilde{\xi}}\phi_{-5.50} \\ - 0.55\ e^{-6.75\widetilde{\xi}}\ \phi_{-6.75} - 0.15\ e^{-7.40\widetilde{\xi}}\phi_{-7.40}\ ,\end{aligned} \tag{4.3b}$$

and

$$\begin{aligned}\phi_{(CC)_1} = -0.70\ e^{0.13\widetilde{\xi}}\ \phi_{0.13} - 0.35\ e^{-0.06\widetilde{\xi}}\phi_{-0.06} \\ - 0.61\ e^{-2.01\widetilde{\xi}}\ \phi_{-2.01} - 0.08\ e^{-5.50\widetilde{\xi}}\phi_{-5.50} \\ + 0.02\ e^{-6.75\widetilde{\xi}}\ \phi_{-6.75} + 0.05\ e^{-7.40\widetilde{\xi}}\phi_{-7.40}\ ,\end{aligned} \tag{4.3c}$$

where $\widetilde{\xi} = \frac{C_F}{\beta}\xi(Q^2)$. We will discuss the second hidden-color state $\phi_{(CC)_2}$ in the next section.

As seen from Eq. (4.3), each distribution amplitude has a distinct high Q^2 behavior which depends on whether it is composed of colorless or colorful clusters. The prototypes of the dibaryon system have a negligible coefficient for the most leading term at high Q^2 and relatively large coefficients for the next-to-leading terms, whereas the hidden color state $(CC)_1$ has a large coefficient for the leading term.

One can imagine constructing a state at the scale Q_0 which only has the NN component of Eq. (4.3a) and then studying its evolution as Q increases. The high Q^2 behavior of $\phi(x_i, Q)$ gives the probability amplitude that all the quarks have impact separation less than $1/Q$. Thus the colorful clusters tend to coexist at short distances; i.e., the colorful clusters tend to attract each other and the colorless clusters tend to repel each other at short distances. Although these results are strictly only applicable in the limit of vanishing interparticle separation, they do provide rigorous constraints on the effective nuclear potential at short distances.

5. ANOMALOUS STATES

In the last section, we expanded the effective two-cluster representations in terms of the eigensolutions of the evolution equation and derived constraints on the effective nuclear potential at short distances. A state which at large distances corresponds to two colorless clusters (such as NN and $\Delta\Delta$) acts as if there is a short-distance repulsive potential between them. On the other hand, a state which consists of two colorful clusters at large distance ($(CC)_1$) sees an attractive potential at short distances. These results show that the leading contribution of QCD to the multiquark wavefunction at short distances has a behavior consistent with the repulsive core nucleon-nucleon potential of conventional nuclear physics.[8] However, we also find that the theory predicts the existence of anomalous states which differ from the normal nuclear degree of freedoms.

As shown in Table III, if the total power n of orbital representation is zero, then only the completely symmetric orbital is possible. Thus, we can read Table III vertically but not horizontally. Since this state cannot exist without including

hidden color components with 50% probability,[9] we cannot interpret this state with normal nucleonic degrees of freedom. If such states exist in physical nuclei then they can provide non-additive nuclear phenomena, such as that observed in the EMC effect[4] in deep inelastic lepton-nucleus structure functions.

The $(CC)_2$ state in the orthonormal cluster basis also has anomalous properties. If we expand the $n = 2$ component in terms of eigensolutions, then

$$\begin{aligned}\phi_{(CC)_2}(x_i, Q) = &- 0.04 e^{0.13\widetilde{\xi}}\, \phi_{0.13} - 0.30 e^{-5.50\widetilde{\xi}}\, \phi_{-5.50} \\ &- 0.95 e^{-7.40\widetilde{\xi}} \phi_{-7.40}\ .\end{aligned} \tag{5.1}$$

Since this state has negligible coefficients for the leading terms and very large coefficient for the strongly damped non-leading terms, the $(CC)_2$ state acts as if there is a repulsive potential between two colorful clusters at short distances. This behavior contrasts with the more conventional behavior of $(CC)_1$

If such a nuclear state were quasi-stable it could have unusual interaction properties. Since it consists of separated triplets (octets in $SU(3)_C$) the state has a large color-dipole moment, producing large hadronic cross sections and short mean free paths. It is amusing to speculate whether the states in QCD analogous to the $(CC)_2$ cluster configurations have any connection with the anomalous phenomena apparently observed in heavy ion collisions.[3,10]

6. SUMMARY AND CONCLUSIONS

The results in this paper represent a first attempt to extract exact results for the composition and interactions of multiquark nuclear systems at short distances. For simplicity, we have analyzed four-quark bound states in $SU(2)_C$, but we expect that many of the derived properties extend to six-quark states in QCD.[11] In particular, since the leading eigensolution at high momentum transfer has 80% hidden color probability,[9] we expect a transition of the ordinary nuclear state to non-nucleonic degrees of freedom as one evolves from long to short distances.

The set of eigensolutions of the evolution equation represent all the possible degrees of freedom of the multiquark bound state system since its kernel has the same invariances and symmetries of the full QCD Hamiltonian. We thus expect that the eigensolutions of the evolution kernel which are dominantly hidden-color to correspond to actual states and excitations of ordinary nuclei. A careful experimental search for these exotic resonances should be made. Possible channels where signals for such states may be observed include Compton and pion photoproduction on a deuteron target at large angles.

REFERENCES

1. S. J. Brodsky and Chueng-Ryong Ji, SLAC-PUB-3076(1985).

2. G. P. Lepage and S. J. Brodsky, Phys. Rev. D 22, 2157 (1980). S. J. Brodsky, SLAC-PUB-3191, published in *Short-distance Phenomena in Nuclear Physics*, D. H. Boal and R. M. Woloshyn eds. Plenum (1983).

3. B. Judek, Can. J. Phys. 46, 343 (1968); 50, 2082 (1972); I. Otterlund, Sixth High Energy Heavy Ion Study and Second Workshop on Anomaly, held at LBL, June 28 to July 1 (1983); E.M.Friedlander et. al., Phys. Rev.Lett. 45, 1084(1980).

4. R. Jaffe, Nature, 296, 305 (1982); E. Gabathuler, Progress in Particle and Nuclear Physics, Vol. 13, Chapter 12, edited by A. Faessler (1985).

5. M. Hammermesh, *Group Theory* (Addison-Wesley, Reading, Mass. 1962).

6. M. Harvey, lectures given at TRIUMF, 20-24 October 1980; H. A. Jahn and H. Van Wieringen, Proc. Roy. Soc. A209, 502 (1951); J. P. Elliott, J. Hope and H. A. Jahn, Phil. Trans. Roy. Soc. 246, 241 (1953).

7. M. Harvey, Nucl. Phys. A352, 301 (1981); A352, 326 (1981).

8. C. Detar, Harvard University Report No. HU-TFT-82-6, 1982 (unpublished); M. Harvey, Ref. 7; R. L. Jaffe, Phys. Rev. Lett. 50, 228 (1983); G. E. Brown, Progress in Particle Nuclear Physics, Vol. 8, Chapter 5, edited by D. Wilkinson (1982); A. Faessler, Progress in Particle and Nuclear Physics, Vol. 13, Chapter 9, edited by A. Faessler (1985).

9. The realistic six-quark state has 80% hidden color state. See S. J. Brodsky, C.-R. Ji and G. P. Lepage, Phys. Rev. Lett. 51, 83 (1983).

10. P. J. S. Watson, Phys. Lett. 126B, 289 (1983); W. J. Romo and P. J. S. Watson, Phys. Lett. 88B, 354 (1979).

11. The six-quark evolution formalism is developed and the leading anomalous dimension of a realistic deuteron are given in Chueng-Ryong Ji and S. J. Brodsky, SLAC-PUB-3148.

TABLE CAPTIONS

Table I: A set of antisymmetric representations for $T = 0$ four-quark distribution amplitude i) $S_Z = 0$ ii) $S_Z = 1$ iii) $S_Z = 2$ case. The normalization factors are given in iv). For simplicity we present the effective representations which are a part of completely antisymmetric representations such as $S_1 T_2$ or $\overline{S}_1 T_2$ terms for i), $(\uparrow\uparrow\uparrow\downarrow)$ T_1 terms for ii), and $(\uparrow\uparrow\uparrow\uparrow)$ T_1 terms for iii).

Table II: Eigenvalues and eigensolutions for $T = 0$ four-quark system up to total orbital power $n = 2$. Every eigensolution is a linear combination of completely antisymmetric representations given by Table 1. For convenience, we represent eigensolutions as Young diagrams of spin and orbital spaces since the color and isospin Young diagram is fixed by $\begin{array}{|c|c|}\hline b & b \\ \hline w & w \\ \hline \end{array} \times \begin{array}{|c|c|}\hline u & u \\ \hline d & d \\ \hline \end{array}$.

Table III: Transition between four-quark antisymmetric representations and effective two-cluster representations. Square and curly brackets represent the orbital (O) and spin-isospin (TS) symmetries respectively.

TABLE I

(i) $S_Z = 0$: S_1T_2 or $\overline{S}_1T_2$ terms

Spin × Orbital (SO)	Effective Representations
$\boxed{\uparrow}\boxed{\uparrow}\boxed{\downarrow}\boxed{\downarrow} \times \boxed{0}\boxed{0}\boxed{0}\boxed{0}$	$\frac{1}{\sqrt{2}}(\varsigma_3 - \varsigma_1)$
$\begin{array}{|c\|c\|}\hline\uparrow&\uparrow\\\hline\downarrow&\downarrow\\\hline\end{array} \times \boxed{0}\boxed{0}\boxed{0}\boxed{0}$	$\frac{1}{\sqrt{2}}(\varsigma_1 - \varsigma_2)$
$\begin{array}{|c\|c\|c\|}\hline\uparrow&\uparrow&\downarrow\\\hline\downarrow\\\cline{1-1}\end{array} \times \begin{array}{|c\|c\|c\|}\hline0&0&0\\\hline1\\\cline{1-1}\end{array} \left(\square\square\square\square\right)$	$\frac{1}{2\sqrt{2}}(\varsigma_3 - \varsigma_1)(x_1 - x_2 + x_3 - x_4)$
$\begin{array}{|c\|c\|c\|}\hline\uparrow&\uparrow&\downarrow\\\hline\downarrow\\\cline{1-1}\end{array} \times \begin{array}{|c\|c\|c\|}\hline0&0&0\\\hline1\\\cline{1-1}\end{array} \left(\begin{array}{|c\|c\|}\hline\ &\ \\\hline\ &\ \\\hline\end{array}\right)$	$\frac{1}{2\sqrt{2}}(\varsigma_1 - \varsigma_2)(x_1 - x_2 + x_3 - x_4)$
$\boxed{\uparrow}\boxed{\uparrow}\boxed{\downarrow}\boxed{\downarrow} \times \boxed{0}\boxed{0}\boxed{1}\boxed{1}$	$\frac{1}{2\sqrt{3}}(\varsigma_3 - \varsigma_1)\left(x_1x_2 + x_1x_3 + x_1x_4 + x_2x_3 + x_2x_4 + x_3x_4 - \frac{1}{3}\right)$
$\begin{array}{|c\|c\|}\hline\uparrow&\uparrow\\\hline\downarrow&\downarrow\\\hline\end{array} \times \boxed{0}\boxed{0}\boxed{1}\boxed{1}$	$\frac{1}{2\sqrt{3}}(\varsigma_1 - \varsigma_2)\left(x_1x_2 + x_1x_3 + x_1x_4 + x_2x_3 + x_2x_4 + x_3x_4 - \frac{1}{3}\right)$
$\begin{array}{|c\|c\|c\|}\hline\uparrow&\uparrow&\downarrow\\\hline\downarrow\\\cline{1-1}\end{array} \times \begin{array}{|c\|c\|c\|}\hline0&0&1\\\hline1\\\cline{1-1}\end{array} \left(\square\square\square\square\right)$	$\frac{1}{2}(\varsigma_3 - \varsigma_1)\left\{x_2x_4 - x_1x_3 + \frac{1}{5}(x_1 - x_2 + x_3 - x_4)\right\}$
$\begin{array}{|c\|c\|c\|}\hline\uparrow&\uparrow&\downarrow\\\hline\downarrow\\\cline{1-1}\end{array} \times \begin{array}{|c\|c\|c\|}\hline0&0&1\\\hline1\\\cline{1-1}\end{array} \left(\begin{array}{|c\|c\|}\hline\ &\ \\\hline\ &\ \\\hline\end{array}\right)$	$\frac{1}{2}(\varsigma_1 - \varsigma_2)\left\{x_2x_4 - x_1x_3 + \frac{1}{5}(x_1 - x_2 + x_3 - x_4)\right\}$
$\begin{array}{|c\|c\|}\hline\uparrow&\uparrow\\\hline\downarrow&\downarrow\\\hline\end{array} \times \begin{array}{|c\|c\|}\hline0&0\\\hline1&1\\\hline\end{array} \left(\square\square\square\square\right)$	$\frac{1}{2\sqrt{6}}(\varsigma_3 - \varsigma_1)\{-x_1x_2 - x_3x_4 - x_1x_4 - x_2x_3 + 2(x_1x_3 + x_2x_4)\}$
$\boxed{\uparrow}\boxed{\uparrow}\boxed{\downarrow}\boxed{\downarrow} \times \begin{array}{|c\|c\|}\hline0&0\\\hline1&1\\\hline\end{array}$	$\frac{1}{2\sqrt{3}}\{\varsigma_1(x_1 - x_2)(x_3 - x_4) + \varsigma_2(x_1 - x_4)(x_2 - x_3) + \varsigma_3(x_1 - x_3)(x_4 - x_2)\}$
$\begin{array}{|c\|c\|}\hline\uparrow&\uparrow\\\hline\downarrow&\downarrow\\\hline\end{array} \times \begin{array}{|c\|c\|}\hline0&0\\\hline1&1\\\hline\end{array} \left(\begin{array}{|c\|c\|}\hline\ &\ \\\hline\ &\ \\\hline\end{array}\right)$	$\frac{1}{2\sqrt{3}}\{\varsigma_1(x_1 - x_4)(x_3 - x_2) + \varsigma_2(x_1 - x_2)(x_4 - x_3) + \varsigma_3(x_1 - x_3)(x_2 - x_4)\}$
$\begin{array}{|c\|c\|}\hline\uparrow&\uparrow\\\hline\downarrow&\downarrow\\\hline\end{array} \times \begin{array}{|c\|c\|}\hline0&0\\\hline1&1\\\hline\end{array} \left(\begin{array}{|c\|}\hline\ \\\hline\ \\\hline\ \\\hline\ \\\hline\end{array}\right)$	$\frac{1}{2\sqrt{6}}(-\varsigma_1 + 2\varsigma_2 - \varsigma_3)(x_1 - x_3)(x_2 - x_4)$

(ii) $S_Z = 1$: $(\uparrow\uparrow\uparrow\downarrow)$ T_1 terms

Spin × Orbital (SO)	Effective Representations
$\begin{array}{|c|c|c|c|}\hline\uparrow&\uparrow&\uparrow&\downarrow\\\hline\end{array} \times \begin{array}{|c|c|c|c|}\hline 0&0&0&0\\\hline\end{array}$	$\frac{1}{\sqrt{2}}(\varsigma_2 - \varsigma_3)$
$\begin{array}{|c|c|c|}\hline\uparrow&\uparrow&\uparrow\\\hline\downarrow\\\cline{1-1}\end{array} \times \begin{array}{|c|c|c|}\hline 0&0&0\\\hline 1\\\cline{1-1}\end{array} \left(\begin{array}{|c|c|c|c|}\hline&&&\\\hline\end{array}\right)$	$\frac{1}{2\sqrt{6}}(\varsigma_2 - \varsigma_3)(-x_1 - x_2 - x_3 + 3x_4)$
$\begin{array}{|c|c|c|}\hline\uparrow&\uparrow&\uparrow\\\hline\downarrow\\\cline{1-1}\end{array} \times \begin{array}{|c|c|c|}\hline 0&0&0\\\hline 1\\\cline{1-1}\end{array} \left(\begin{array}{|c|c|}\hline&\\\hline&\\\hline\end{array}\right)$	$\frac{1}{\sqrt{6}}\{\varsigma_1(x_1 - x_3) + \varsigma_2(x_2 - x_1) + \varsigma_3(x_3 - x_2)\}$
$\begin{array}{|c|c|c|c|}\hline\uparrow&\uparrow&\uparrow&\downarrow\\\hline\end{array} \times \begin{array}{|c|c|c|c|}\hline 0&0&1&1\\\hline\end{array}$	$\frac{1}{2\sqrt{3}}(\varsigma_2 - \varsigma_3)\left(x_1x_2 + x_1x_3 + x_1x_4 + x_2x_3 + x_2x_4 + x_3x_4 - \frac{1}{3}\right)$
$\begin{array}{|c|c|c|}\hline\uparrow&\uparrow&\uparrow\\\hline\downarrow\\\cline{1-1}\end{array} \times \begin{array}{|c|c|c|}\hline 0&0&1\\\hline 1\\\cline{1-1}\end{array} \left(\begin{array}{|c|c|c|c|}\hline&&&\\\hline\end{array}\right)$	$\frac{1}{2\sqrt{3}}(\varsigma_2 - \varsigma_3)\left\{x_1x_2 + x_1x_3 - x_1x_4 + x_2x_3 - x_2x_4 - x_3x_4 + \frac{1}{5}(-x_1 - x_2 - x_3 + 3x_4)\right\}$
$\begin{array}{|c|c|c|}\hline\uparrow&\uparrow&\uparrow\\\hline\downarrow\\\cline{1-1}\end{array} \times \begin{array}{|c|c|c|}\hline 0&0&1\\\hline 1\\\cline{1-1}\end{array} \left(\begin{array}{|c|c|}\hline&\\\hline&\\\hline\end{array}\right)$	$\frac{1}{2\sqrt{3}}\left[\varsigma_1\left\{-x_1x_2 + x_3x_4 - x_1x_4 + x_2x_3 + \frac{2}{5}(x_1 - x_3)\right\} + \varsigma_2\left\{-x_2x_4 + x_1x_3 + x_1x_4 - x_2x_3 + \frac{2}{5}(-x_1 + x_2)\right\} + \varsigma_3\left\{x_1x_2 - x_3x_4 + x_2x_4 - x_1x_3 + \frac{2}{5}(-x_2 + x_3)\right\}\right]$
$\begin{array}{|c|c|c|c|}\hline\uparrow&\uparrow&\uparrow&\downarrow\\\hline\end{array} \times \begin{array}{|c|c|}\hline 0&0\\\hline 1&1\\\hline\end{array}$	$\frac{1}{2\sqrt{3}}\{\varsigma_1(x_1 - x_3)(x_4 - x_2) + \varsigma_2(x_1 - x_2)(x_3 - x_4) + \varsigma_3(x_1 - x_4)(x_2 - x_3)\}$

(iii) $S_Z = 2$: ($\uparrow\uparrow\uparrow\uparrow$) T_1 terms

Spin × Orbital	Effective Representations
$\boxed{\uparrow}\boxed{\uparrow}\boxed{\uparrow}\boxed{\uparrow} \times \boxed{0}\boxed{0}\boxed{0}\boxed{0}$	$\frac{1}{\sqrt{2}}(\varsigma_2 - \varsigma_3)$
$\boxed{\uparrow}\boxed{\uparrow}\boxed{\uparrow}\boxed{\uparrow} \times \boxed{0}\boxed{0}\boxed{1}\boxed{1}$	$\frac{1}{2\sqrt{3}}(\varsigma_2 - \varsigma_3)\left(x_1x_2 + x_1x_3 + x_1x_4 + x_2x_3 + x_2x_4 + x_3x_4 - \frac{1}{3}\right)$
$\boxed{\uparrow}\boxed{\uparrow}\boxed{\uparrow}\boxed{\uparrow} \times \begin{array}{|c|c|}\hline 0&0\\\hline 1&1\\\hline\end{array}$	$\frac{1}{2\sqrt{3}}\{\varsigma_1(x_1 - x_3)(x_4 - x_2) + \varsigma_2(x_1 - x_2)(x_3 - x_4) + \varsigma_3(x_1 - x_4)(x_2 - x_3)\}$

(iv) Normalization Factors: For every representations, the following normalization constants must be multiplied according to their orbital representations.

Orbital	Normalization
$\boxed{0}\boxed{0}\boxed{0}\boxed{0}$	$\sqrt{7!}$
$\begin{array}{|c|c|c|}\hline 0&0&0\\\hline 1\\\cline{1-1}\end{array}$	$6\sqrt{7!}$
$\boxed{0}\boxed{0}\boxed{1}\boxed{1}$	$6\sqrt{165} \times \sqrt{7!}$
$\begin{array}{|c|c|c|}\hline 0&0&1\\\hline 1\\\cline{1-1}\end{array}$	$10\sqrt{33} \times \sqrt{7!}$
$\begin{array}{|c|c|}\hline 0&0\\\hline 1&1\\\hline\end{array}$	$6\sqrt{55} \times \sqrt{7!}$

TABLE II

	$b_n[\gamma_n = (2+b_n)C_F/\beta]$	Spin × Orbit (SO)
$S_z = 0$	$-\frac{8}{3}$	$\frac{1}{\sqrt{2}}\left(\begin{array}{|c|c|c|c|}\hline\uparrow&\uparrow&\downarrow&\downarrow\\\hline\end{array} - \begin{array}{|c|c|}\hline\uparrow&\uparrow\\\hline\downarrow&\downarrow\\\hline\end{array}\right) \times \begin{array}{|c|c|c|c|}\hline 0&0&0&0\\\hline\end{array}$
	-2.13	$0.56\left(\begin{array}{|c|c|c|c|}\hline\uparrow&\uparrow&\downarrow&\downarrow\\\hline\end{array} - \begin{array}{|c|c|}\hline\uparrow&\uparrow\\\hline\downarrow&\downarrow\\\hline\end{array}\right) \times \begin{array}{|c|c|c|c|}\hline 0&0&1&1\\\hline\end{array} - 0.43 \begin{array}{|c|c|c|c|}\hline\uparrow&\uparrow&\downarrow&\downarrow\\\hline\end{array} \times \begin{array}{|c|c|}\hline 0&0\\\hline 1&1\\\hline\end{array}$
		$+ \begin{array}{|c|c|}\hline\uparrow&\uparrow\\\hline\downarrow&\downarrow\\\hline\end{array} \times \begin{array}{|c|c|}\hline 0&0\\\hline 1&1\\\hline\end{array} \left(0.32 \begin{array}{|c|c|c|c|}\hline\end{array} - 0.03 \begin{array}{|c|c|}\hline\\\hline\\\hline\end{array} - 0.28 \begin{array}{|c|}\hline\\\hline\\\hline\\\hline\end{array}\right)$
	-1.94	$-0.22\left(\begin{array}{|c|c|c|c|}\hline\uparrow&\uparrow&\downarrow&\downarrow\\\hline\end{array} + \begin{array}{|c|c|}\hline\uparrow&\uparrow\\\hline\downarrow&\downarrow\\\hline\end{array}\right) \times \begin{array}{|c|c|c|c|}\hline 0&0&1&1\\\hline\end{array} + 0.28 \begin{array}{|c|c|c|c|}\hline\uparrow&\uparrow&\downarrow&\downarrow\\\hline\end{array} \times \begin{array}{|c|c|}\hline 0&0\\\hline 1&1\\\hline\end{array}$
		$+ \begin{array}{|c|c|}\hline\uparrow&\uparrow\\\hline\downarrow&\downarrow\\\hline\end{array} \times \begin{array}{|c|c|}\hline 0&0\\\hline 1&1\\\hline\end{array} \left(-0.24 \begin{array}{|c|c|c|c|}\hline\end{array} - 0.61 \begin{array}{|c|c|}\hline\\\hline\\\hline\end{array} - 0.63 \begin{array}{|c|}\hline\\\hline\\\hline\\\hline\end{array}\right)$
	$-\frac{2}{9}$	$\begin{array}{|c|c|c|}\hline\uparrow&\uparrow&\downarrow\\\hline\downarrow\\\cline{1-1}\end{array} \times \begin{array}{|c|c|c|}\hline 0&0&1\\\hline 1\\\cline{1-1}\end{array} \left(\frac{1}{\sqrt{2}} \begin{array}{|c|c|c|c|}\hline\end{array} - \frac{1}{\sqrt{2}} \begin{array}{|c|c|}\hline\\\hline\\\hline\end{array}\right)$
	0	$\frac{1}{\sqrt{2}}\left(\begin{array}{|c|c|c|c|}\hline\uparrow&\uparrow&\downarrow&\downarrow\\\hline\end{array} + \begin{array}{|c|c|}\hline\uparrow&\uparrow\\\hline\downarrow&\downarrow\\\hline\end{array}\right) \times \begin{array}{|c|c|c|c|}\hline 0&0&0&0\\\hline\end{array}$
	0	$\begin{array}{|c|c|c|}\hline\uparrow&\uparrow&\downarrow\\\hline\downarrow\\\cline{1-1}\end{array} \times \begin{array}{|c|c|c|}\hline 0&0&0\\\hline 1\\\cline{1-1}\end{array} \left(\frac{1}{\sqrt{2}} \begin{array}{|c|c|c|c|}\hline\end{array} + \frac{1}{\sqrt{2}} \begin{array}{|c|c|}\hline\\\hline\\\hline\end{array}\right)$
	0.006	$-0.47\left(\begin{array}{|c|c|c|c|}\hline\uparrow&\uparrow&\downarrow&\downarrow\\\hline\end{array} + \begin{array}{|c|c|}\hline\uparrow&\uparrow\\\hline\downarrow&\downarrow\\\hline\end{array}\right) \times \begin{array}{|c|c|c|c|}\hline 0&0&1&1\\\hline\end{array} + 0.40 \begin{array}{|c|c|c|c|}\hline\uparrow&\uparrow&\downarrow&\downarrow\\\hline\end{array} \times \begin{array}{|c|c|}\hline 0&0\\\hline 1&1\\\hline\end{array}$
		$+ \begin{array}{|c|c|}\hline\uparrow&\uparrow\\\hline\downarrow&\downarrow\\\hline\end{array} \times \begin{array}{|c|c|}\hline 0&0\\\hline 1&1\\\hline\end{array} \left(0.53 \begin{array}{|c|c|c|c|}\hline\end{array} + 0.35 \begin{array}{|c|c|}\hline\\\hline\\\hline\end{array} - 0.03 \begin{array}{|c|}\hline\\\hline\\\hline\\\hline\end{array}\right)$
	$\frac{8}{9}$	$\begin{array}{|c|c|c|}\hline\uparrow&\uparrow&\downarrow\\\hline\downarrow\\\cline{1-1}\end{array} \times \begin{array}{|c|c|c|}\hline 0&0&0\\\hline 1\\\cline{1-1}\end{array} \left(-\frac{1}{\sqrt{2}} \begin{array}{|c|c|c|c|}\hline\end{array} + \frac{1}{\sqrt{2}} \begin{array}{|c|c|}\hline\\\hline\\\hline\end{array}\right)$

$\frac{10}{3}$

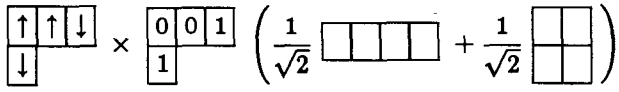

3.5

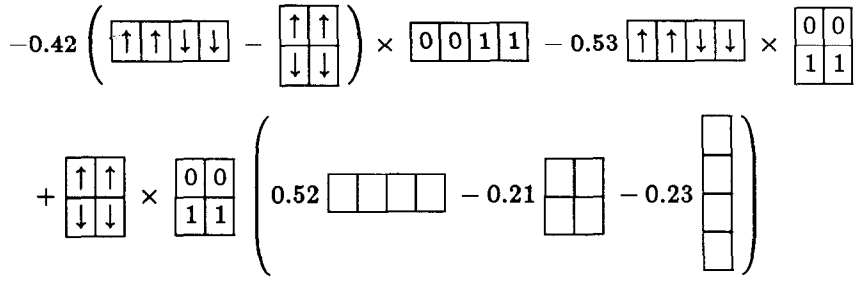

4.75

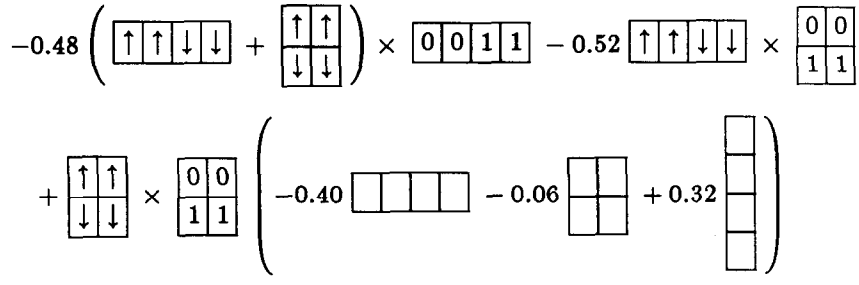

5.40

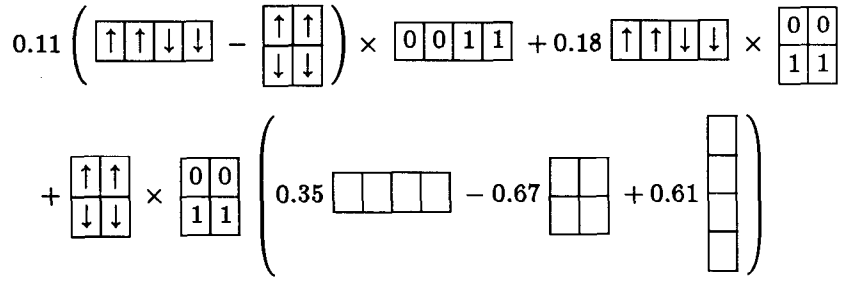

$S_z = 1$

$\frac{11-\sqrt{1033}}{18}$

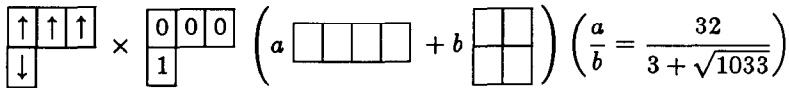

-1

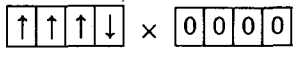

-0.98

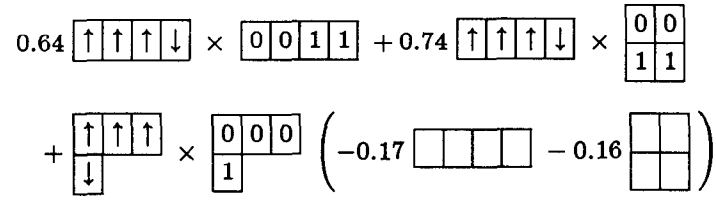

1.13

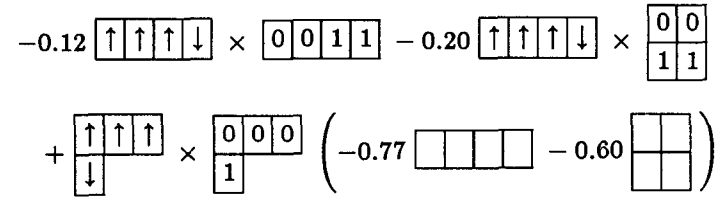

	$\frac{11+\sqrt{1033}}{18}$	$\begin{array}{|c|c|c|}\hline\uparrow&\uparrow&\uparrow\\\hline\downarrow\\\cline{1-1}\end{array} \times \begin{array}{|c|c|c|}\hline 0&0&0\\\hline 1\\\cline{1-1}\end{array} \left(-b \begin{array}{|c|c|c|c|}\hline&&&\\\hline\end{array} + a \begin{array}{|c|c|}\hline&\\\hline&\\\hline\end{array}\right)$
	2.51	$0.04 \begin{array}{|c|c|c|c|}\hline\uparrow&\uparrow&\uparrow&\downarrow\\\hline\end{array} \times \begin{array}{|c|c|c|c|}\hline 0&0&1&1\\\hline\end{array} - 0.07 \begin{array}{|c|c|c|c|}\hline\uparrow&\uparrow&\uparrow&\downarrow\\\hline\end{array} \times \begin{array}{|c|c|}\hline 0&0\\\hline 1&1\\\hline\end{array}$
		$+ \begin{array}{|c|c|c|}\hline\uparrow&\uparrow&\uparrow\\\hline\downarrow\\\cline{1-1}\end{array} \times \begin{array}{|c|c|c|}\hline 0&0&0\\\hline 1\\\cline{1-1}\end{array} \left(0.62 \begin{array}{|c|c|c|c|}\hline&&&\\\hline\end{array} - 0.78 \begin{array}{|c|c|}\hline&\\\hline&\\\hline\end{array}\right)$
	4.4	$0.76 \begin{array}{|c|c|c|c|}\hline\uparrow&\uparrow&\uparrow&\downarrow\\\hline\end{array} \times \begin{array}{|c|c|c|c|}\hline 0&0&1&1\\\hline\end{array} - 0.64 \begin{array}{|c|c|c|c|}\hline\uparrow&\uparrow&\uparrow&\downarrow\\\hline\end{array} \times \begin{array}{|c|c|}\hline 0&0\\\hline 1&1\\\hline\end{array}$
		$+ \begin{array}{|c|c|c|}\hline\uparrow&\uparrow&\uparrow\\\hline\downarrow\\\cline{1-1}\end{array} \times \begin{array}{|c|c|c|}\hline 0&0&0\\\hline 1\\\cline{1-1}\end{array} \left(-0.02 \begin{array}{|c|c|c|c|}\hline&&&\\\hline\end{array} + 0.09 \begin{array}{|c|c|}\hline&\\\hline&\\\hline\end{array}\right)$
$S_z = 2$	0	$\begin{array}{|c|c|c|c|}\hline\uparrow&\uparrow&\uparrow&\uparrow\\\hline\end{array} \times \begin{array}{|c|c|c|c|}\hline 0&0&0&0\\\hline\end{array}$
	0	$\begin{array}{|c|c|c|c|}\hline\uparrow&\uparrow&\uparrow&\uparrow\\\hline\end{array} \times \left(\sqrt{\frac{4}{7}} \begin{array}{|c|c|c|c|}\hline 0&0&1&1\\\hline\end{array} - \sqrt{\frac{3}{7}} \begin{array}{|c|c|}\hline 0&0\\\hline 1&1\\\hline\end{array}\right)$
	$\frac{14}{3}$	$\begin{array}{|c|c|c|c|}\hline\uparrow&\uparrow&\uparrow&\uparrow\\\hline\end{array} \times \left(\sqrt{\frac{3}{7}} \begin{array}{|c|c|c|c|}\hline 0&0&1&1\\\hline\end{array} + \sqrt{\frac{4}{7}} \begin{array}{|c|c|}\hline 0&0\\\hline 1&1\\\hline\end{array}\right)$

TABLE III

	[4]{22}	[22]{22}	[22]{4}	[22]{1111}
NN	$-\frac{1}{2}$	$-\frac{1}{2}$	$\frac{1}{\sqrt{2}}$	0
$\Delta\Delta$	$\frac{1}{2}$	$\frac{1}{2}$	$\frac{1}{\sqrt{2}}$	0
$(CC)_1$	$\frac{1}{\sqrt{2}}$	$-\frac{1}{\sqrt{2}}$	0	0
$(CC)_2$	0	0	0	1

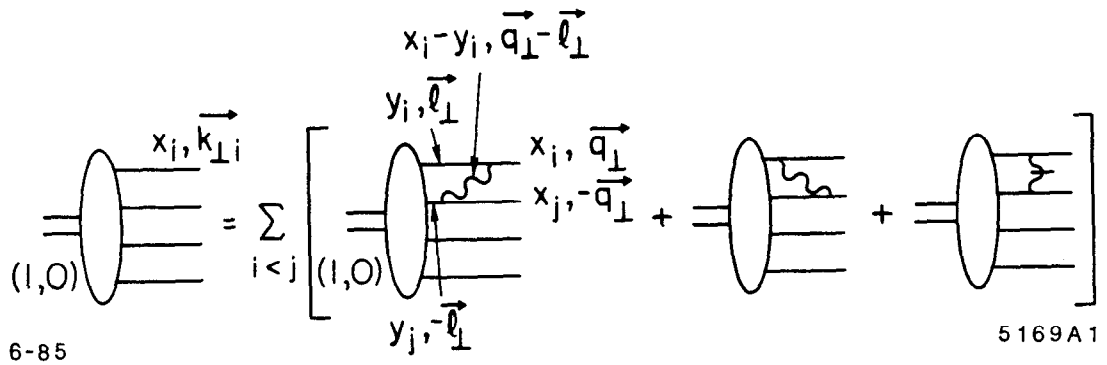

Figure 1: Evolution equation for the four-quark wave function to leading order in $\alpha_s(Q^2)$.